Kidney International, Vol. 59 (2001), pp. 1424–1431

Dietary zinc deficiency increases uroguanylin accumulation in rat kidney

Li Cui, Raymond K. Blanchard, and Robert J. Cousins

Food Science and Human Nutrition Department and Center for Nutritional Sciences, University of Florida, Gainesville, Florida, USA

Dietary zinc deficiency increases uroguanylin accumulation in rat kidney.

Background. Zinc deficiency in humans produces a secretory diarrhea that is corrected by zinc supplementation. In rats, differential mRNA display analysis has shown that intestinal uroguanylin gene expression is increased in zinc deficiency. An endocrine axis involving intestinal uroguanylin and the kidney may exist. Therefore, we conducted this study to examine whether zinc deficiency would affect uroguanylin expression in the kidney of rats.

Methods. A purified diet, deficient or adequate in zinc content, was fed to rats. Preprouroguanylin mRNA was localized in kidney by in situ hybridization, and prouroguanylin/uroguanylin peptides were localized in the kidney by immunohistochemistry. Abundance was measured by Western blotting and slot blotting analyses.

Results. In situ hybridization demonstrated that preprouroguanylin mRNA-expressing cells were localized in the proximal tubules, being primarily limited to the cortical-medullary junction. Zinc deficiency did not alter the abundance or distribution of the mRNA. Immunohistochemistry, using a uroguanylin peptide-specific, affinity-purified antibody, demonstrated that immunoreactive uroguanylin peptide was localized to the same cells but that the staining was stronger in zinc-deficient rats. Western blotting analysis of kidney extracts showed that there was no difference in abundance of prouroguanylin between zinc adequate and deficient rats. However, slot blotting analysis demonstrated that the abundance of a low molecular weight immunoreactive peptide, presumably uroguanylin, was higher in extracts of zinc-deficient rats.

Conclusion. The results suggest that production of prouroguanylin by the kidney, in contrast to the intestine, is not influenced by dietary zinc intake, but that higher amounts of uroguanylin in kidney extracts may reflect renal processing of the hormone obtained from the systemic circulation.

Uroguanylin, an intestinal natriuretic hormone [1], has unique biochemical and pharmacological properties [2–6]. Endogenous uroguanylin stimulates the transepithelial secretion of both Cl^- and HCO_3^- anions in the intestine [7, 8], while circulating uroguanylin and prouroguanylin are involved in regulation of urinary NaCl excretion [9, 10] through activating guanylate cyclase receptors in the gastrointestinal epithelium and kidney [11–14].

Uroguanylin has been isolated from urine, blood, and small intestine samples from human, opossum, and rat [2–4, 12]. Uroguanylin mRNA is very abundant in the proximal small intestine of rats, with progressively decreasing amounts in the lower small intestine and colon [15]. The gene is also expressed in the thymus, stomach, pancreas, lung, testis, and kidney, albeit at very much lower levels [3, 4, 15]. In situ hybridization evidence shows that the cells in mouse kidney that express uroguanylin mRNA were located at the region between the cortex and the medulla, but detailed cell localizations were not provided [16]. Immunohistochemical studies showed that uroguanylin is located in the proximal tubules of rat kidney [17], and the proximal and distal tubules as well as the collecting ducts, but not in the glomeruli or renal vasculature in human kidney [18]. Renal uroguanylin expression argues for a function for the hormone in the kidney.

It has been hypothesized that an endocrine axis exists, involving uroguanylin released from the gastrointestinal tract into the circulation [19]. The experiments conducted by Lennane et al demonstrated that oral NaCl loads elicit a much larger increase in urinary Na^+ excretion than that caused by intravenous salt, suggesting that induction of uroguanylin in the gastrointestinal tract may play a role at the kidney level [20]. Furthermore, circulating uroguanylin levels are increased with the severity of chronic renal disease, and correlate with water and sodium retention. Consequently, uroguanylin may participate in a novel endocrine axis linking the intestine and the kidney as a physiological mechanism that influences body sodium and water homeostasis [19]. The kidney also may serve as the route for uroguanylin elimination. Therefore, the reduced functioning renal mass and de-

Key words: diarrhea, endocrine axis, renal proximal tubules, natriuretic peptide.

Received for publication August 15, 2000
and in revised form October 27, 2000
Accepted for publication November 3, 2000

creased glomerular filtration seen in renal disease may account for the increase in uroguanylin observed in renal disease.

Our previous study demonstrated that dietary zinc deficiency up-regulates uroguanylin mRNA levels in the small intestine [15]. Recently, we further demonstrated that zinc deficiency caused overproduction of prouroguanylin peptide in the intestine [21]. Increased uroguanylin precursor peptide production in the intestine may lead to an increase of the bioactive form of the hormone in the circulation. The present studies were conducted with rats to see whether zinc deficiency could affect renal prouroguanylin expression and the renal abundance of uroguanylin peptides.

METHODS

Zinc-deficient diet studies

Male Sprague-Dawley rats (Harlan, Indianapolis, IN, USA) weighing 150 to 175 g were individually housed and fed an AIN-76a–based pelleted diet as described previously [21, 22]. All rats received the zinc-adequate diet (30 mg Zn/kg) for one week. Thereafter, one half of the rats continued to receive the same diet, while the other half received one modified to provide <1 mg Zn/kg for 15 days. A pair-fed group was not included in these experiments since it was shown previously that uroguanylin expression is not significantly influenced by food restriction [15]. The rats were anesthetized with methoxyflurane and killed by exsanguination between 0900 and 1200 hours. Blood was collected by cardiac puncture, and the serum zinc concentration ($N = 5$ per group) was measured by flame atomic absorption spectrophotometry [22]. A total of 18 rats was used in preliminary and principal experiments. All animal procedures were approved by the University of Florida Institutional Animal Care and Use Committee.

In situ hybridization

Tissues were processed for in situ hybridization as described previously [21]. Briefly, renal tissues were immediately fixed with buffered 4% paraformaldehyde and sealed in paraffin, and 4 μm sections were mounted. These were washed twice with xylene and then 95% and 70% ethanol, followed with phosphate-buffered saline (PBS) containing 0.3% Triton X-100. Sections were permeabilized with proteinase K (20 μg/mL; Roche, Indianapolis, IN, USA) in 100 mmol/L Tris-HCl, 50 mmol/L ethylenediaminetetraacetic acid (EDTA), pH 8.0, fixed with 4% paraformaldehyde, and washed twice with PBS. After incubation with 0.1 mol/L triethanolamine (pH 8.0) containing 0.25% (vol/vol) acetic anhydride, the sections were incubated with prehybridization buffer [4 × standard saline citrate (SSC), 50% (vol/vol) deionized formamide].

Hybridization was performed overnight in 50% deionized formamide, 10% dextran sulfate, 1 × Denhardt's solution, 4 × SSC, 10 mmol/L dithiothreitol, 1 mg/mL yeast tRNA, 1 mg/mL denatured sheared salmon sperm DNA, and approximately 200 ng/mL of labeled RNA probe. These probes were derived from a rat prepro-uroguanylin clone containing the 3′ end of the cDNA [15] that was linearized with HindIII or Xbal prior to in vitro transcription with SP6 and T7 RNA polymerases and digoxigenin reagents (Roche). As a control, sense and antisense probes were always applied to adjacent sections. After hybridization, sections were washed sequentially in 2 × SSC, 1 × SSC plus 50% formamide, and buffer 1 (100 mmol/L Tris, pH 7.5, 150 mmol/L NaCl). Blocking to preclude nonspecific hybridization was in buffer 2 (buffer 1 containing 0.1% Triton X100 and 2% normal sheep serum). Next, a 1:10 dilution of a fluorescein-conjugated antidigoxigenin antibody (Roche) or, alternatively, a 1:500 dilution of an alkaline phosphatase-conjugated antidigoxigenin antibody (Roche) in buffer 1 or buffer 2, respectively, was added. The sections in which the former antibody was used were viewed immediately. The sections where the latter antibody was used were washed twice in buffer 1 at room temperature and incubated in 100 mmol/L Tris (pH 9.5), 100 mmol/L NaCl, and 50 mmol/L $MgCl_2$. Color development was stopped by washing with 10 mmol/L Tris-HCl (pH 8.1), 1 mmol/L EDTA, followed briefly with distilled water, and sections were then viewed. Sections were counterstained with fast green FcF (0.02%; Fisher Biotech, Fair Lawn, NJ, USA).

Photomicrographs were obtained with an Axiovert S100 fluorescence microscope (Carl Zeiss, Thornwood, NY, USA) equipped with a SPOT digital CCD camera (Diagnostic Instruments, Sterling Heights, MI, USA) for image analysis.

Western blot and dot blot experiments

For quantitative Western analysis, the kidney was immediately homogenized in four volumes of 20 mmol/L HEPES (pH 7.4), 1 mmol/L EDTA, and 300 mmol/L mannitol, containing 5% protease inhibitor cocktail (P2714; added immediately before use; Sigma, St. Louis, MO, USA). Following centrifugation at 225,000 × g, the cytosolic fraction was collected and analyzed by Lowry assay [23] for protein content. Equal amounts of cytosolic protein (300 μg) were resolved on a 15% Tris/tricine sodium dodecyl sulfate-polyacrylamide gel electrophoresis (SDS-PAGE) [24] and electroblotted onto Immobilon-P (Millipore, Bedford, MA, USA) using 192 mmol/L glycine, 10 mmol/L Tris, 0.05% SDS, 20% methanol. The membranes were incubated with affinity-purified (AP) antibody after being blocked with 5% nonfat dry milk in PBS-T (150 mmol/L PBS; 0.05% Tween-20, pH 7.5). After washing with PBS-T, anti-rabbit IgG horse-

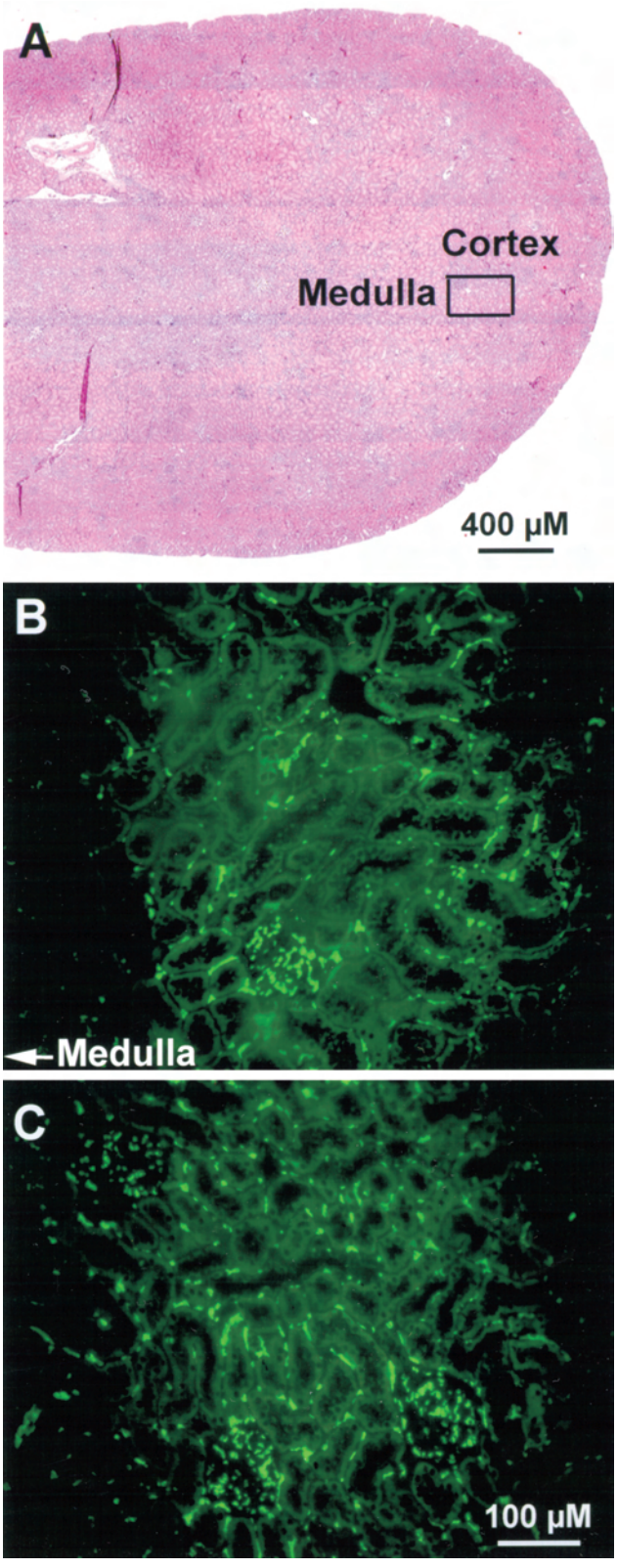

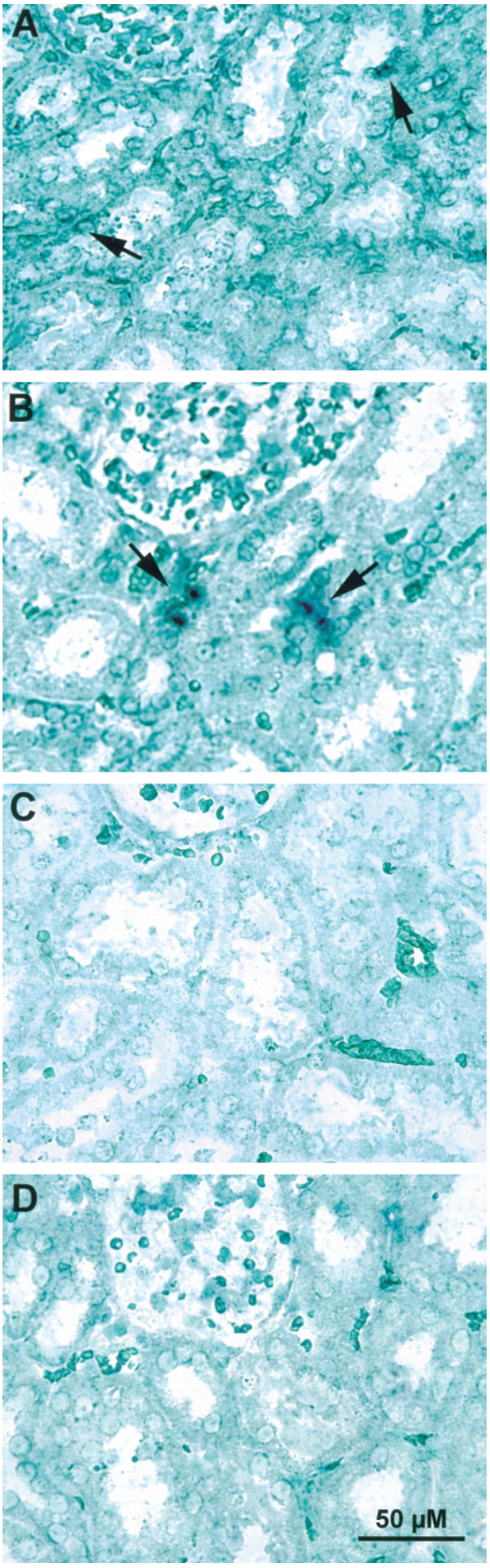

Fig. 1. In situ hybridizations showing the anatomic distribution of uroguanylin mRNA transcripts in the kidney. The section of kidney examined is indicated by the box shown in (*A*). The fluorescein-conjugated antisense riboprobe used for detection of the mRNA displayed fluorescence signals predominantly in the region between the cortex and the medulla (*B* and *C*). A representative section from the zinc-adequate rats is shown in (B), while one from the zinc deficient rats is shown in (C). The bars are 400 microns (μM) (A) or 100 microns (μM) (B and C).

radish peroxidase conjugate (Sigma) was applied for detection by Renaissance® Chemiluminescence (NEN, Boston, MA, USA). The antibody was generated in rabbits from a uroguanylin peptide (TDECELCINVACTGC) composed of all three disulfide conformations according to mass spectrometry analysis and was conjugated to keyhole limpet hemocyanin by glutaraldehyde. Finally, the antibody was purified from the IgG fraction by affinity chromatography using the uroguanylin peptide [21].

To estimate uroguanylin levels, tissue samples were prepared as described previously in this article. Kidney cytosol (80 μL) was placed in Microcon-3 concentrators (cut off 3 kD; Amicon, Inc., Beverly, MA, USA). Centrifugation with four washes using the homogenization buffer was at 3500 × *g* for four hours (4°C). Equal amounts of cytosolic protein (300 μg) in the filtrate were applied to a nitrocellulose membrane using a slot blot apparatus. After incubation with antibody as mentioned previously in this article, a chemiluminescence substrate (SuperSignal® West Femto Maximum Sensitivity Substrate; Pierce, Rockford, IL, USA) that produces an intensified signal was used for immunodetection.

Immunohistochemistry

A Histostain™-SP Kit (Zymed Laboratories, Inc., South San Francisco, CA, USA) was used for immunohistochemical detection. After deparaffinizing and hydration, the sections were incubated in 3% H_2O_2, rinsed with PBS-T, and then blocked with 10 g/L bovine serum albumin (BSA) and 10% normal goat serum. Finally, they were incubated overnight at 4°C with the AP uroguanylin antibody (1:100 = 10 μg/mL) or flowthrough elute (FT) from affinity purification (negative control), both diluted in 1% normal goat serum/PBS. After washing, sections were incubated with biotinylated goat anti-rabbit IgG at room temperature, rinsed, and streptavidin-peroxidase conjugate was added to develop the red 3-amino-9-ethylcarbazole chromagen (AEC). Counterstaining was performed by using hematoxylin before mounting. Histologic morphology was demonstrated using hematoxylin and eosin staining.

Statistical analysis

Data are expressed as means ± SD. Differences between groups were determined using a two-tailed Student *t* test. A value of $P < 0.05$ was considered to be significant.

RESULTS

Rats fed the zinc-deficient diet for 15 days had lower body weights and weight gain compared with controls (data not shown). The concentration of zinc in serum was significantly lower ($P < 0.01$) in zinc-deficient than in zinc-adequate rats (0.21 ± 0.03 vs. 1.11 ± 0.03 μg/mL, means ± SD, respectively).

A histologic section of kidney, indicating where the tissue used for in situ hybridization was obtained, is shown in Figure 1A. Hybridization using the prepro-uroguanylin antisense riboprobe showed that the mRNA signals from the fluorescein-conjugated antidigoxigenin antibody under the low-power magnification were primarily distributed in the cells localized to the cortical-medullary junction (Fig. 1B, C). Feeding the zinc-deficient diet for 15 days (Fig. 1C) did not appear to alter the intensity and location of uroguanylin mRNA in the kidney compared with zinc-adequate rats (Fig. 1B). Comparable sections in which the sense probe was used did not show any specific staining (data not shown). The alkaline phosphatase-conjugated antidigoxigenin antibody did not produce a distinct signal at the same magnification (data not shown), possibly because of the sensitivity difference of the fluorimetric versus colorimetric methods. However, under high-power magnification, the alkaline phosphatase-conjugated antisense riboprobe showed a signal in the renal proximal tubular cells (Fig. 2A, B). As with the fluorimetric method, there was no apparent difference between zinc-deficient (Fig. 2B) and zinc-adequate (Fig. 2A) rats. Comparable sections in which the sense probe was used did not show any specific staining (Fig. 2C, D).

Western blot analysis demonstrated that the affinity purified (AP) antibody clearly recognized a protein of about 8 kD (presumably prouroguanylin) in the kidney cytosol (Fig. 3). Furthermore, the amount of prouroguanylin protein was not markedly changed by zinc deficiency. In contrast, slot blot analysis showed that a low molecular weight (<3 kD) immunoreactive species, presumably uroguanylin, was greatly elevated in the kidney of zinc-deficient rats compared with that of zinc-adequate rats (Fig. 4).

Using low magnification (×100), the positive staining against the uroguanylin-specific antibody was predominantly distributed in the cortical-medullary junction of the kidney in zinc-adequate rats (Fig. 5A). Zinc deficiency strongly enhanced the intensity of the positive

Fig. 2. In situ hybridization showing the distribution of uroguanylin mRNA transcripts in the kidney using the alkaline phosphatase-conjugated riboprobe. Preprouroguanylin mRNA signals using the antisense probe are primarily localized in renal proximal tubular cells (as shown by the arrows). Representative sections from zinc adequate rats are shown in *A* and *C*, while those from zinc deficient rats are shown in *B* and *D*. There was no specific signal using the uroguanylin sense riboprobe in place of the antisense riboprobe (C and D). The bar is equivalent to 50 microns (μM).

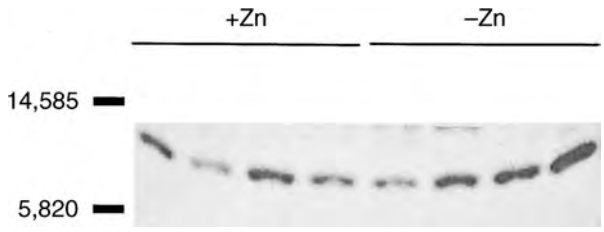

Fig. 3. Western blot analysis demonstrating prouroguanylin abundance in the kidney. Renal cytosolic proteins were separated by 15% Tris/tricine SDS-PAGE and electroblotted to nylon membrane. The uroguanylin affinity-purified antibody recognizes a band of about 8 kD in the cytosol derived from the kidneys of individual zinc-deficient (−Zn) and zinc-adequate (+Zn) rats (N = 4 per dietary group).

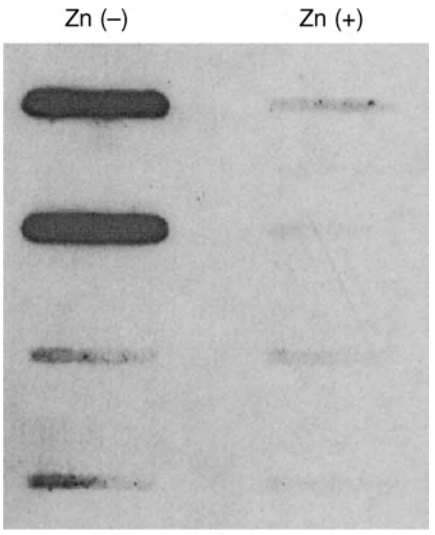

Fig. 4. Slot blot analysis demonstrating abundance of immunoreactive small peptides (<3 kD), presumably uroguanylin, in the kidney. Samples of kidney cytosol derived from individual rats were processed with Microcon-3 concentrators to obtain peptides of <3 kD. Equal amounts of cytosolic peptide (300 mg) were applied to a nitrocellulose membrane using a slot blot apparatus. The blots were visualized by high sensitivity chemiluminescence using the same detection antibody as in Figure 3. The protein applied to each slot was derived from the kidney of individual zinc-deficient (−Zn) and zinc-adequate (+Zn) rats (N = 4 per dietary group).

staining, but did not alter the distribution (Fig. 5B). There was no specific staining when the FT was used in place of the uroguanylin-specific AP antibody (data not shown). At a higher magnification (×630), the renal proximal tubular cells (marked with arrows) showed pronounced staining for uroguanylin (Fig. 6). Zinc-deficient rats (Fig. 6C) showed a much stronger intensity of uroguanylin-specific staining in the renal proximal tubular cells compared with those of zinc-adequate rats (Fig. 6A) when stained for the same length of time. No uroguanylin-specific staining was found in the distal tubules, glomerulus, or medulla of the kidney (Fig. 6A, C). Furthermore, there was no positive staining using the FT in place of the antibody (Fig. 6B, D).

A comparison between conventional histologic staining and both in situ hybridization and immunohistochemical staining using high magnification is shown in Figure 7. Hematoxylin and eosin-stained sections are shown in Figure 7A and B. The signals produced with the antisense riboprobe for preprouroguanylin mRNA were limited to the cytoplasm close to the nucleus in the proximal tubular cells, with comparable signals in tissue from both zinc-adequate and zinc-deficient rats (Fig. 7C, D). However, the positive staining against uroguanylin/prouroguanylin peptides produced using the AP antibody was extensively distributed in the renal proximal tubular cells, spreading from the brush border to the basolateral membrane (Fig. 7E, F).

DISCUSSION

This study presents the novel finding that zinc deficiency causes uroguanylin accumulation in the kidney. The quantity of uroguanylin, but not of prouroguanylin, appeared to be increased in the kidney, particularly in the proximal tubular cells of zinc-deficient rats. Results of in situ hybridization of preprouroguanylin mRNA and of Western blotting analysis of the precursors of the hormone peptide suggest that the increase of uroguanylin may mainly come from the circulation, since there was no difference in the abundance of uroguanylin mRNA or precursor peptide in kidneys of zinc-adequate and zinc-deficient rats.

A synthetic peptide of 15 residues from the carboxy terminal of rat uroguanylin, confirmed by mass spectometry to have all three possible disulfide conformations, was used to prepare the rabbit polyclonal antibody for the present study. Previous characterization demonstrated that immunoreactivity of the immune serum, total IgG fraction, and AP fraction was uroguanylin peptide-specific since neither the preimmune serum nor unbound IgG fraction from affinity purification exhibited reactivity [21]. The specificity was also confirmed by incubating the AP antibody with uroguanylin peptide prior to Western analysis. This abolished the 8 kD protein band. The location of this protein band on Western blotting analysis is consistent with another report from separate investigators [25]. However, the mature 15 aa peptide is approximately 1.575 kD and is not detectable under current Western blot conditions. While this peptide is retained on the gel during electrophoresis under our conditions, the inability of small peptides to be retained efficiently by the membrane during electroblotting does not allow for effective transfer. In an attempt to circumvent this difficulty, in some experiments, the cytosol used for Western analysis was passed through a Microcon-3 membrane (3 kD cut-off; Millipore), and the filtrate was slot blotted to a nitrocellulose membrane

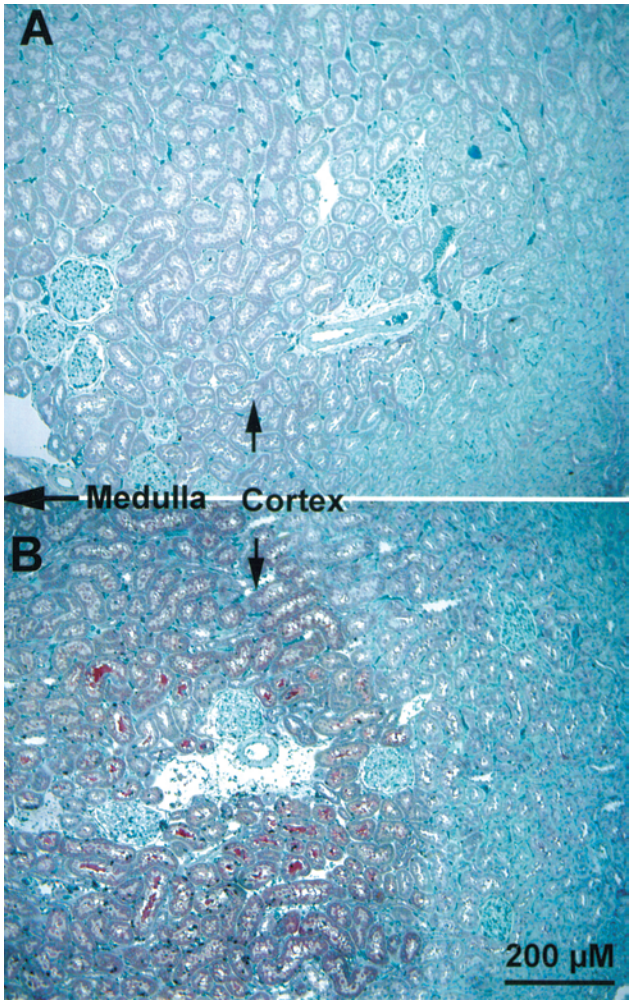

Fig. 5. Immunohistochemistry showing the anatomic distribution of uroguanylin/prouroguanylin peptides in the kidney. Specific staining was localized predominantly in the region between the cortex and the medulla using a uroguanylin AP antibody as shown in these representative sections (*A* and *B*). Zinc-deficient rat kidney showed a stronger intensity of the immunoreactivity (*B*) compared with that of a zinc-adequate rat using the same staining time (A). The bar is 200 microns (μM).

prior to immunodetection, as was done for the Western blots. Signals were detected that presumably represent terminally cleaved uroguanylin because peptides larger than 3 kD had been excluded during the ultrafiltration process.

The present data demonstrate that there is variation in the abundance of uroguanylin peptide in kidney (Figs. 3 and 4) within each group. The two-week dietary feeding period was chosen in the present study because, in our experience, this treatment does not produce gross changes such as tissue zinc concentrations or in cell morphology [15, 21, 22]. Zinc concentration in the serum decreased by approximately 80% using the two-week protocol. However, there were rather high inner group variations (twofold to fourfold) in the serum zinc concentration even if zinc deficiency was overwhelming [26]. The serum concentration of zinc ranged from 0.15 to 0.30 μg/mL in the present study, which could account for the variation in uroguanylin abundance if the two are mechanistically linked. In addition, intake of water is not traditionally controlled in the zinc-deficient model. The daily intake of water in zinc-deficient animals varied between 2 and 17 mL, and administration of N^G-nitro-L-arginine methyl ester, a nitric oxide synthase inhibitor, did not change water intake [27, 28]. Therefore, it is expected that daily urine output amount varies individually in parallel to the daily intake of water. To establish a link with uroguanylin peptide accumulation in the kidney, a direct observation of daily intake and output is needed in a future study.

The results presented in this report demonstrate that uroguanylin mRNA and protein are primarily distributed in the cells localized to the cortical-medullary junction, which is consistent with a previous report [16]. This anatomical site contains juxtamedullary nephrons, which are essential for establishing the gradient of hypertonicity to produce hypertonic urine [29]. Immunohistochemical studies show that positive uroguanylin staining is localized in the proximal tubular cells and possibly those in the thick descending limb. The histologic location suggests that receptors for uroguanylin are located in the apical membrane of the proximal tubules [17, 18].

Uroguanylin levels in plasma and/or in urine increased in congestive heart failure [30], glomerulonephritis [31], and the nephritic syndrome [32], showing a common relationship to body water and sodium homeostasis. In these studies, it could not be concluded whether decreased clearance of the peptide was due to a reduced functioning renal mass and decreased glomerular filtration rates or an increase in production of the peptide owing to renal dysfunction mediated as a consequence of enteric uroguanylin release into the circulation. Our results argue for a pathway where the additional uroguanylin produced in the gastrointestinal tract during zinc deficiency is deposited in the kidney as a consequence of elevation in the circulating level rather than being an outcome of renal damage. This seems likely since the two-week protocol of zinc deficiency in the present study does not cause gross changes in cell morphology in the kidney or produce any other indicators of kidney damage. On the other hand, depletion of dietary zinc for two weeks results in an imbalance in distribution of multiple elements in various organs and tissues [33]. Taken together, the uroguanylin level in the circulation and/or urine may serve as a clinical marker, indicating imbalance in body water and sodium homeostasis, and possibly as a secondary marker for zinc deficiency.

In conclusion, zinc deficiency increases uroguanylin accumulation in the proximal tubules of kidney in rats. The increase of uroguanylin peptide, the active form of

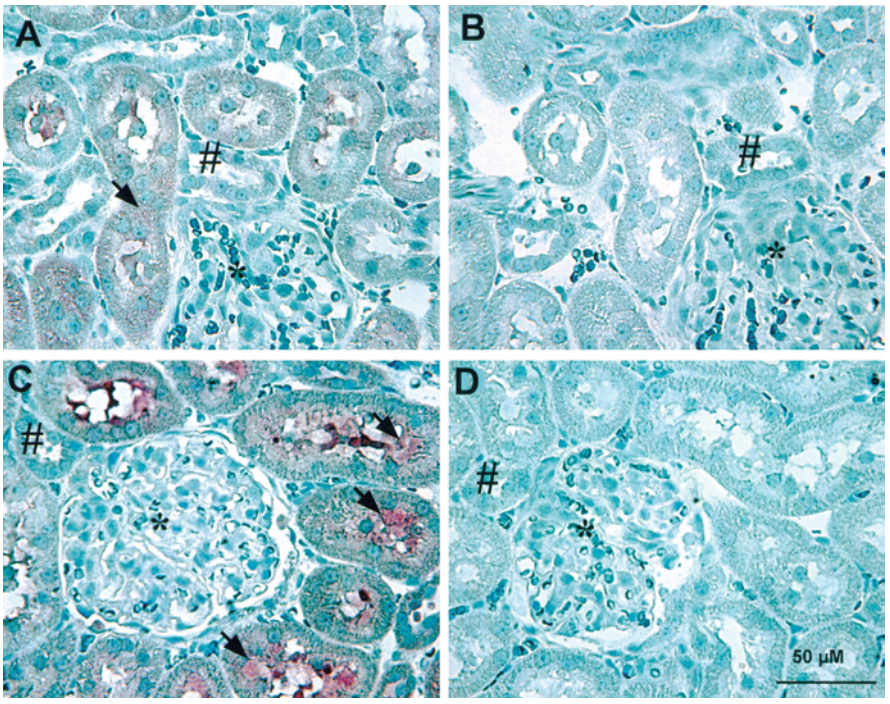

Fig. 6. Immunohistochemistry showing the cellular distribution of uroguanylin/prouroguanylin peptides in the kidney. Specific staining was localized primarily in the proximal tubular cells using the uroguanylin AP antibody as shown in these representative sections (*A* and *C*). Sections from zinc-deficient rats showed a stronger intensity of the immunoreactivity (C) compared with that of zinc-adequate rats in the same staining time (A). Little nonspecific staining was observed using the unbound flow-through (FT) fraction from affinity purification in place of the AP antibody (*B* and *D*). Symbols are: (↑) proximal tubule; (#) distal tubule; (*) glomerulus. The bar is 50 microns (μM).

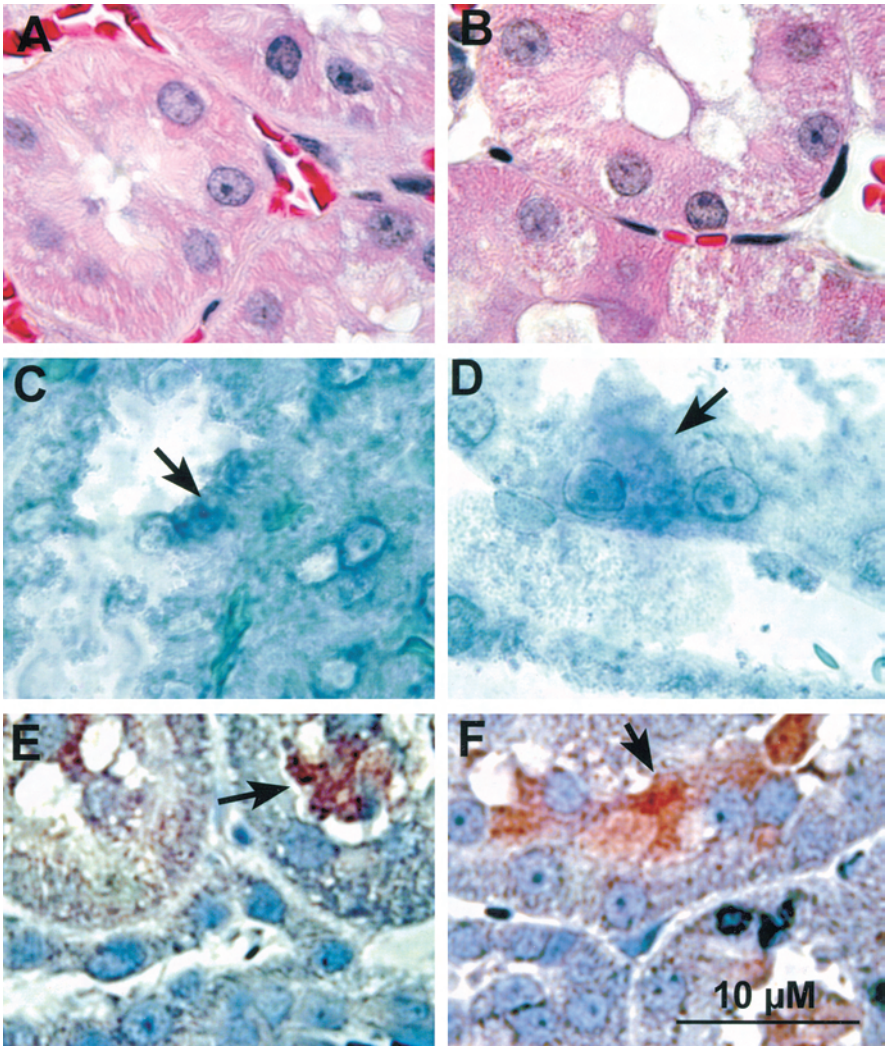

Fig. 7. Comparison between cellular location of preprouroguanylin mRNA and uroguanylin/prouroguanylin peptides. (*A* and *B*) Hematoxylin and eosin-stained kidney sections from zinc-adequate and zinc-deficient rats, respectively. The mRNA signals from in situ hybridization were found in the cytoplasm close to the nucleus in the proximal tubular cells in both zinc-adequate (*C*) and zinc-deficient (*D*) rats. However, the immunoreactivity of the peptides was rather extensively distributed in cells, spreading from the brush border to the basolateral membrane (*E* and *F*, respectively). The positive staining is indicated by an arrow. The bar is 10 microns (μM).

the hormone, compared with the precursor prouroguanylin and the location of uroguanylin deposition suggests a physiological and/or pathophysiological function in the kidney that may relate to the water imbalance observed during zinc deficiency.

ACKNOWLEDGMENTS

Research described in this article was supported by National Institutes of Health Grants DK 52412 and DK 31127 and by the Boston Family Endowment Funds of the University of Florida. This paper is part of Florida Agricultural Experimental Station Journal Series No. R-07863.

Reprint requests to Dr. Robert J. Cousins, Food Science and Human Nutrition Department, University of Florida, 201 FSHN, P.O. Box 110370, Gainesville, Florida 32611-0370, USA.
E-mail: rjc@gnv.ifas.ufl.edu

REFERENCES

1. Forte LR: Guanylin regulatory peptides: Structures, biological activities mediated by cyclic GMP and pathobiology. *Regul Pept* 81:25–39, 1999
2. Kita T, Smith CE, Fok KF, *et al:* Characterization of human uroguanylin: A member of the guanylin peptide family. *Am J Physiol* 266:F342–F348, 1994
3. Fan X, Hamra FK, London RM, *et al:* Structure and activity of uroguanylin and guanylin from the intestine and urine of rats. *Am J Physiol* 273:E957–E964, 1997
4. Li Z, Perkins AG, Peters MF, *et al:* Purification, cDNA sequence, and tissue distribution of rat uroguanylin. *Regul Pept* 68:45–56, 1997
5. Hamra FK, Krause WJ, Eber SL, *et al:* Opossum colonic mucosa contains uroguanylin and guanylin peptides. *Am J Physiol* 270: G708–G716, 1996
6. Wiegand RC, Kato J, Currie MG: Rat guanylin cDNA characterization of the precursor of an endogenous activator of intestinal guanylate cyclase. *Biochem Biophys Res Commun* 185:812–817, 1992
7. Hill O, Cetin Y, Cieslak A, *et al:* A new human guanylate cyclase-activating peptide (GCAP-II, uroguanylin): Precursor cDNA and colonic expression. *Biochim Biophys Acta* 1253:146–149, 1995
8. Guba M, Kuhn M, Forssmann WG, *et al:* Guanylin strongly stimulates rat duodenal HCO_3^- secretion: Proposed mechanism and comparison with other secretagogues. *Gastroenterology* 111:1558–1568, 1996
9. Fan X, Hamra FK, Freeman RH, *et al:* Uroguanylin: Cloning of preprouroguanylin cDNA, mRNA expression in the intestine and heart and isolation of uroguanylin and prouroguanylin from plasma. *Biochem Biophys Res Commun* 219:457–462, 1996
10. Forte LR, Fan X, Hamra FK: Salt and water homeostasis: Uroguanylin is a circulating peptide hormone with natriuretic activity. *Am J Kidney Dis* 28:296–304, 1996
11. Currie MG, Fox KF, Kato J, *et al:* Guanylin: An endogenous activator of intestinal guanylate cyclase. *Proc Natl Acad Sci USA* 89:947–951, 1992
12. Hamra FK, Forte LR, Eber SL, *et al:* Uroguanylin: Structure and activity of a second endogenous peptide that stimulates intestinal guanylate cyclase. *Proc Natl Acad Sci USA* 90:10464–10468, 1993
13. Forte LR, Krause WJ, Freeman RH: *Escherichia coli* enterotoxin receptors: Localization in opossum kidney, intestine, and testis. *Am J Physiol* 257:F874–F881, 1989
14. London RM, Krause WJ, Fan X, *et al:* Signal transduction pathways via guanylin and uroguanylin in stomach and intestine. *Am J Physiol* 273:G93–G105, 1997
15. Blanchard RK, Cousins RJ: Upregulation of rat intestinal uroguanylin mRNA by dietary zinc restriction. *Am J Physiol* 272: G972–G978, 1997
16. Whitaker TL, Witte DP, Scott MC, *et al:* Uroguanylin and guanylin: Distinct but overlapping patterns of messenger RNA expression in mouse intestine. *Gastroenterology* 113:1000–1006, 1997
17. Nakazato M, Yamaguchi H, Date Y, *et al:* Tissue distribution, cellular source, and structural analysis of rat immunoreactive uroguanylin. *Endocrinology* 139:5247–5254, 1998
18. Fujimoto S, Kinoshita H, Hara S, *et al:* Immunohistochemical localization of uroguanylin in the human kidney. *Nephron* 84:88–89, 2000
19. Forte LR, London RM, Freeman RH, *et al:* Guanylin peptides: Renal actions mediated by cyclic GMP. *Am J Physiol* 278:F180–F191, 2000
20. Lennane RJ, Peart WS, Carey RM, *et al:* A comparison on natriuresis after oral and intravenous sodium loading in sodium-depleted rabbits: Evidence for a gastrointestinal or portal monitor of sodium intake. *Clin Sci Mol Med* 49:433–436, 1975
21. Cui L, Blanchard RK, Coy LM, *et al:* Prouroguanylin overproduction and localization in the intestine of zinc-deficient rats. *J Nutr* 130:2726–2732, 2000
22. Blanchard RK, Cousins RJ: Differential display of intestinal mRNAs regulated by dietary zinc. *Proc Natl Acad Sci USA* 93: 6863–6868, 1996
23. Lowry OH, Rosebrough NJ, Farr AL, *et al:* Protein measurements with Folin phenol reagent. *J Biol Chem* 193:266–275, 1951
24. Hempe JM, Cousins RJ: Cysteine-rich intestinal protein and intestinal metallothionein: An inverse relationship as a conceptual model for zinc absorption in rats. *J Nutr* 122:89–95, 1992
25. Perkins A, Goy MF, Li Z: Uroguanylin is expressed by enterochromaffin cells in the rat gastrointestinal tract. *Gastroenterology* 113: 1007–1014, 1997
26. Cui L, Takagi Y, Nezu R, *et al:* Prolonged zinc-deficient diet alters alkaline phosphatase and disaccharidase activities and induces morphological changes in the intestine of rats. *J Trace Elem Exp Med* 8:249–261, 1996
27. Cui L, Takagi Y, Sando K, *et al:* Nitric oxide synthase inhibitor attenuates intestinal damage induced by zinc deficiency in rats. *J Nutr* 129:792–798, 1999
28. Cui L, Takagi Y, Sando K, *et al:* Nitric oxide synthase inhibitor attenuates inflammatory lesions in the skin of zinc deficient rats. *Nutrition* 16:34–41, 2000
29. Junqueira LC, Carneiro J, Kelley RO: The urinary system, in *Basic Histology* (8th ed), edited by Junqueira LC, Carneiro J, Kelley RO, Norwalk, Appleton and Lange, 1995, pp 359–377
30. Carrithers SL, Eber SL, Forte LR, *et al:* Increased urinary excretion of uroguanylin in patients with congestive heart failure. *Am J Physiol* 278:H538–H547, 2000
31. Kinoshita H, Fujimoto S, Nakazato M, *et al:* Urine and plasma levels of uroguanylin and its molecular forms in renal diseases. *Kidney Int* 52:1028–1034, 1997
32. Kinoshita H, Fujimoto S, Fukae H, *et al:* Plasma and urine levels of uroguanylin, a new natriuretic peptide, in nephrotic syndrome. *Nephron* 81:160–164, 1999
33. Gupta RP, Verma PC, Sadana JR, *et al:* Effect of experimental zinc deficiency and repletion on sodium, potassium, copper and iron concentrations in guinea-pigs. *Br J Nutr* 62:407–414, 1989